

THE STRAIN ENERGY OF A DISK-SHAPED GP ZONE

Contents

Abstract . . . . .	v
I. Introduction . . . . .	1
II. Theoretical Considerations . . . . .	4
A. Khachaturyan's Solution . . . . .	4
B. Strain Energy of Disk-Shaped Inclusions . . . . .	6
C. Evaluation of the Computational Parameters . . . . .	7
III. Results on Strain Energy Calculations . . . . .	10
A. Dependence of the Specific Strain Energy on Elastic Properties . . . . .	10
B. Dependence of the Specific Strain Energy in $\epsilon_p$ and $\epsilon_n$ . . . . .	13
IV. Discussion . . . . .	14
A. Relationship Between Minimum Energy Orientations and Elastic Anisotropy . . . . .	14
B. The Case for Al-Cu . . . . .	14
C. The Case for Cu-Be . . . . .	15
D. General Discussion . . . . .	16
V. Conclusions . . . . .	18
Acknowledgements . . . . .	19
References . . . . .	20
Figure Captions . . . . .	21
Figures . . . . .	23

NOTICE

This report was prepared as an account of work sponsored by the United States Government. Neither the United States nor the United States Atomic Energy Commission, nor any of their employees, nor any of their contractors, subcontractors, or their employees, makes any warranty, express or implied, or assumes any legal liability or responsibility for the accuracy, completeness or usefulness of any information, apparatus, product or process disclosed, or represents that its use would not infringe privately owned rights.

MASTER

THE STRAIN ENERGY OF A DISK-SHAPED GP ZONE

John Arthur Wert

Inorganic Materials Research Division, Lawrence Berkeley Laboratory and  
Department of Materials Science and Engineering, College of Engineering;  
University of California, Berkeley, California

ABSTRACT

A simplified form of Khachaturyan's solution to the general problem of determining the strain energy of an arbitrarily-shaped coherent inclusion is found for the case of a disk-shaped inclusion. Specific strain energies are calculated as a function of the orientation of such an inclusion in lattices possessing various elastic properties. Some numerical results are presented. The salient features of the specific strain energy surface are found to depend only on the elastic properties of the lattice. From this a relationship between an elastic anisotropy parameter,  $A$ , and the minimum strain energy orientation of a disk-shaped inclusion is observed. The strain energies of GP zones in Al-Cu and Cu-Be age hardening alloys are calculated. The minimum strain energy orientations of GP zones in these alloys are identical with experimentally observed orientations.

## I. INTRODUCTION

Clusters of solute atoms often formed during the first stage of solid solution decomposition in age hardening alloys are usually referred to as Guinier-Preston (GP) zones. GP zones are coherent with the surrounding matrix phase, thus any difference in atomic spacing between the precipitate and matrix phases will result in coherency strain fields around the clusters. An additional interfacial energy must be associated with the clusters because of the composition variation at the precipitate-matrix interface. Due to anisotropies in crystal lattices, the energies associated with the strain fields and interfaces may be dependent upon the configuration (shape and orientation) of the GP zones. In some cases, a significant contribution to the configuration dependent energy may also be due to interactions between the strain fields of nearby clusters. Generally, however, the other energy changes accompanying GP zone formation are configuration independent. Neglecting the strain field interaction term, one would expect GP zones to form preferentially in configurations which minimize a combination of the strain and additional interfacial energies, thereby minimizing the free energy of the solute atom clusters.

Let us briefly examine the qualitative arguments which relate the shape of GP zones to the size difference between solute and solvent atoms.<sup>1,2</sup> In cases where the solute and solvent atoms are similar in size (to within a few percent) the strain fields of the clusters are relatively weak. The additional interfacial energy is thus the dominating factor and it is minimized by the formation of spherical GP zones. Examples of binary alloy systems in which such clusters are observed are Al-Ag<sup>3</sup> and Cu-Co<sup>4</sup>. If the size difference is appreciable, however, the

energy associated with the coherency strain field of a cluster is considerably larger. In these cases, an increase in the additional interfacial energy is sacrificed to obtain an even larger decrease in the strain energy and disk-shaped GP zones are energetically favored. The best-known examples of this type of behavior are Al-Cu<sup>5</sup> and Cu-Be<sup>6</sup>. In other precipitating systems, notably Al-Mg and Fe-Mo,<sup>17</sup> the size difference is quite large. The beginnings of GP zone formation are observed in such cases but growth is arrested at a very early stage. It has been suggested that this is due to the mechanism by which solute atoms are transported to the clusters.<sup>7,8</sup> For a more complete understanding of the shape of solute atom clusters, additional factors may also be considered, such as the anisotropy of the elastic properties of the crystal.

While the shape of GP zones is seen to depend largely on the relative magnitudes of the strain and additional interfacial energies, the preferred orientation of disk-shaped clusters depends on the anisotropies of these terms (this question is obviously irrelevant in the case of spherical clusters). Schwellinger, Leamy and Warlimont<sup>10</sup> have considered the specific strain energy associated with a two-dimensionally infinite misfitting precipitate sheet in a cubic lattice. Their calculations indicate the existence of a relationship between the elastic anisotropy of the precipitate lattice and the minimum strain energy orientation of the infinite plane. In their analysis, however, deformations normal to the precipitate plane do not contribute to the strain energy and no strains arise in the matrix surrounding the precipitate sheet. Strains in the matrix, especially in the direction normal to the precipitate disk, are a prominent feature of GP zone formation and it is expected that they would

contribute significantly to the total strain energy. The purpose of this study is to examine the anisotropy of the strain energy associated with finite disk-shaped GP zones.

For calculation of the strain energy of a coherent precipitate, two approaches are available. Eshelby<sup>11</sup> obtained a solution in terms of tabulated elliptic integrals for the somewhat restricted case of an ellipsoidal inclusion in an isotropic elastic medium. A slightly more general solution was subsequently obtained by Khachaturyan<sup>12</sup> for the general case of an arbitrarily shaped coherent inclusion in an elastic medium of arbitrary anisotropy.

Presented here are the results of a study of the strain energies associated with disk-shaped GP zones using Khachaturyan's solution. Strain energies are calculated as a function of the orientation of a hypothetical GP zone in various materials. The relationship between the minimum energy orientations and the elastic properties of the material found by Schwallinger et al<sup>10</sup> is seen to be valid for disk-shaped coherent precipitates of finite size.

## II. THEORETICAL CONSIDERATIONS

### A. Khachatryan's Solution

Khachatryan<sup>12</sup> obtained a solution of the general problem of determining the elastic strain energy of a new-phase coherent inclusion of arbitrary shape in an elastic medium of arbitrary anisotropy. The assumptions inherent in this solution require that the inclusion be isolated in an infinite elastic medium and that the elastic properties of the inclusion be identical with those of the surrounding matrix. The latter is equivalent to the assumption that the modulus effect is small with respect to the size effect.

Of primary importance in Khachatryan's solution of this strain energy problem is a tensor which shall be referred to as the free state strain tensor. Consider the volume which is to undergo transformation. Suppose it is removed from the elastic medium and allowed to transform free of the constraints normally imposed on it by this medium. The strains corresponding to the deformations it undergoes as it transforms in the absence of mechanical constraints define the matrix elements of the free state strain tensor.

Khachatryan's solution to this problem may be expressed in the following form:

$$E = \frac{1}{2} \lambda_{ijkl} \epsilon_{ij}^0 \epsilon_{ln}^0 V_T - \frac{1}{2} \int \frac{d^3k}{(2\pi)^3} |\hat{\theta}(k)|^2 A(k) \quad (1)$$

where  $E$  is the strain energy of the coherent inclusion,  $\lambda_{ijkl}$  is the elastic modulus tensor,  $\epsilon_{ij}^0$  is the free state strain tensor,  $V_T$  is the volume which undergoes transformation and  $\hat{\theta}(k)$  are the Fourier components of  $\theta(r)$ , the form function ( $\theta(r)$  being equal to zero outside the inclusion and one

inside it).  $A(\underline{k})$  is defined by the following equation:

$$A(\underline{k}) = (\hat{\sigma}^{\circ} \underline{k}, \hat{G}^{-1} \hat{\sigma}^{\circ} \underline{k})$$

where  $(\dots, \dots)$  is the scalar vector product and  $\hat{G}^{-1}$  is the Green's Function of the elastic equilibrium equation for the inclusion. The matrix elements of the operator  $\hat{\sigma}^{\circ}$  are determined by the relationship

$$[\hat{\sigma}^{\circ}]^{ij} + \lambda_{ijkl} \epsilon^{\circ}_{lm} = 0.$$

Finally, the matrix elements of the operator  $\hat{G}^{-1}$  are defined by the equations

$$[\hat{G}]^{ij} = \lambda_{ijkl} k_l k_m$$

$$\text{and } \hat{G}^{-1} \hat{G} = 1$$

where  $[\hat{1}]^{ij} = \delta_{ij}$ . In all of the above equations (and throughout this paper) summation over repeated indices is implied.

As has been pointed out by Khachatryan,<sup>12</sup> the quantity  $A(\underline{k})$  is actually independent of the magnitude of the vector  $\underline{k}$ . This is because all of the matrix elements of the operator  $\hat{G}^{-1}$  are proportional to  $k^{-2}$  and  $\hat{\sigma}^{\circ}$  is independent of  $k$ . Therefore, the functional form  $A(\underline{k})$  may be replaced by the form  $A\left(\frac{\underline{k}}{k}\right)$  which is dependent upon the direction but not the magnitude of  $\underline{k}$ . Khachatryan thus re-expresses Eq. (1) in the form

$$E = \frac{1}{2} \lambda_{ijkl} \epsilon^{\circ}_{ij} \epsilon^{\circ}_{lm} v_T - \frac{1}{2} \int \frac{d^3 \underline{k}}{(2\pi)^3} |\hat{\theta}(\underline{k})|^2 A \frac{\underline{k}}{k}. \quad (2)$$

This is the general form of Khachatryan's solution to this strain energy problem. While the solution exists in principle, evaluation of Eq.(2) in the general case is difficult. A simplified expression may be obtained, however, for the special case of a disk-shaped inclusion.

B. Strain Energy of Disk-Shaped Inclusions

Consider the Fourier components of the form function in the case of a disk-shaped inclusion. The only non-zero components lie in a direction very nearly parallel to the normal vector of the disk. Thus, as was pointed out by Khachatryan,<sup>12</sup> for such inclusions only  $\underline{k}$  vectors which are nearly parallel to this normal vector will contribute significantly to the integral in Eq. (2). The validity of this approximation depends, of course, on the thickness to diameter ratio of the precipitate disk. In the case of disk-shaped GP zones, the thickness to diameter ratio is generally less than 0.07 and the approximation is very good.

If  $A\left(\frac{\underline{k}}{k}\right)$  is a smooth and slowly varying function of  $\left(\frac{\underline{k}}{k}\right)$ , by the above argument only a slight approximation will be incurred by replacing  $A\left(\frac{\underline{k}}{k}\right)$  with  $A(\underline{n})$ , where  $\underline{n}$  is a unit vector normal to the plane of the inclusion.  $A(\underline{n})$  being constant, it may be removed from the integral and the elastic energy of the disk-shaped inclusion may be re-expressed as:

$$E = \frac{1}{2} \lambda_{ijkl} \epsilon_{ij}^{\circ} \epsilon_{lm}^{\circ} v_T - \frac{A(\underline{n})}{2} \int \frac{d^3 \underline{k}}{(2\pi)^3} |\theta(\underline{k})|^2.$$

This may be further simplified by making use of the identity:

$$v_T = \int \frac{d^3 \underline{k}}{(2\pi)^3} |\theta(\underline{k})|^2.$$

Thus, in the case of a disk-shaped inclusion, Khachatryan re-expressed Eq. (2) in the much simplified form:

$$E = \frac{v_T}{2} \left\{ \lambda_{ijkl} \epsilon_{ij}^{\circ} \epsilon_{lm}^{\circ} - A(\underline{n}) \right\} \quad (3)$$

Numerical evaluation techniques were used to show that  $A\left(\frac{\underline{k}}{k}\right)$  is, in fact, a smooth and slowly varying function of  $\left(\frac{\underline{k}}{k}\right)$  so that the error introduced by the above approximation is very small.



### C. Evaluation of the Calculational Parameters

From Eq. (3) it is immediately obvious that the strain energy of a disk-shaped coherent precipitate is directly proportional to the volume of the precipitate prior to transformation,  $V_T$ . Thus, the parameter of interest is the specific strain energy of the inclusion,  $\frac{E}{V_T}$ , which shall be denoted  $\epsilon_V$ . The parameters required for calculation of  $\epsilon_V$  for a GP zone in a cubic lattice are three independent elastic constants;  $C_{11}$ ,  $C_{12}$  and  $C_{44}$ , the matrix elements of the free state strain tensor and two parameters characterizing the orientation of the disk in the lattice. To see how these parameters are related to measurable quantities, consideration of a model of disk-shaped GP zones in binary alloys is necessary.

X-ray studies<sup>13</sup> and, more recently, high resolution electron microscopy<sup>5,6</sup> have suggested that the model proposed by Gerold<sup>14</sup> best describes the nature of GP zones in Al-Cu and Cu-Be alloys. This model, originally describing the GP zones which form in Al-Cu age hardening alloys, assumes that they are composed of a monolayer of Cu atoms in a matrix of nearly pure Al. Assuming that Gerold's model may be employed to describe GP zones in all binary alloys, the parameters required for the calculation of  $\epsilon_V$  are evaluated as follows in the case of a supersaturated solution of B in A.

The matrix surrounding a fully grown cluster in an A-B alloy is nearly pure A and it may be assumed that the residual concentration of B has only a slight effect on the elastic properties of the A matrix. The most readily accessible elastic constants appropriate to this case are those of pure A.

Prior to transformation, the disk-shaped volume to be transformed contains a more or less random A-B solution. After the GP zone has formed,

it contains pure B. In the unconstrained state, deformations must thus take place in the plane of the disk to change the lattice parameter from that of the A-B solid solution to that appropriate to a monolayer of B. Denote the strain corresponding to free state deformations in the plane of the disk  $\epsilon_p$ . Similar deformations may be imagined in the direction normal to the precipitate disk. The strain corresponding to this deformation is denoted  $\epsilon_n$ .

The free state strain tensor for a GP zone lying in the (001) matrix plane is easily seen to have the following matrix elements

$$\left( \epsilon_{ij} \right)_{001} = \begin{pmatrix} \epsilon_p & 0 & 0 \\ 0 & \epsilon_p & 0 \\ 0 & 0 & \epsilon_n \end{pmatrix}$$

Assuming that the values of the transformation parameters ( $\epsilon_p$  and  $\epsilon_n$ ) are isotropic, the free state strain tensor for a GP zone in any orientation may easily be obtained using coordinate transformation techniques. There remains only the evaluation of the transformation parameters  $\epsilon_p$  and  $\epsilon_n$ .

Lattice parameter measurements, traditionally used to determine atomic misfits, may not be used directly in this case since the stable crystal structures of the A-B solid solution and pure B are not necessarily the same. If the transformation parameters are assumed to be isotropic, the cube root of the volume per atom,  $L_v$ , may be used as a measure of atomic size as well as the efficiency of atomic packing. The change in  $L_v$  from an A-B random solution to pure B is a measure of the free state deformation which must occur in the plane of the disk during the transformation. The strain,  $\epsilon_p$ , corresponding to this deformation is:

$$\epsilon_p = \frac{L_v(B) - L_v(A-B)}{L_v(A-B)} .$$

Along the axis normal to the plane of the precipitate disk one might reasonably suppose that after the transformation,  $L_v$  would be similar to that of a solid solution containing A and B in equal concentrations. The value of  $L_v$  for such a solid solution may be obtained by extrapolation of measured lattice parameters. The strain,  $\epsilon_n$ , along the direction normal to the plane of the disk is thus given by:

$$\epsilon_n = \frac{L_v(\text{extra AB}) - L_v(A-B)}{L_v(A-B)} .$$

In cases where the crystal structures of the A-B solid solution and pure B are the same, this method is equivalent to the direct use of the lattice parameter measurements.

### III. RESULTS OF STRAIN ENERGY CALCULATIONS

#### A. Dependence of the Specific Strain Energy on Elastic Properties

Calculations from lattice parameter measurements<sup>15</sup> for a variety of age hardening alloy systems in which disk-shaped GP zones form have shown that the absolute values of  $\epsilon_p$  and  $\epsilon_n$  generally fall between 0.04 and 0.15. In addition, the value of  $\epsilon_n$  is usually somewhat smaller than that of  $\epsilon_p$ . For investigation of the dependence of the specific strain energy on the elastic properties of the matrix, the values of the transformation parameters will be fixed at  $\epsilon_p = 0.10$  and  $\epsilon_n = 0.07$ . All calculations referred to in this section employed these values of  $\epsilon_p$  and  $\epsilon_n$ .

The specific strain energy was calculated as a function of GP zone orientation using the elastic constants corresponding to several different metals. It is not suggested that disk-shaped GP zones are observed in alloys based on all of these metals, they have been used for comparison purposes only. Some of the results are plotted in Fig. 1 through 6. In these plots, the direction associated with the radial vector is parallel to the GP zone normal and its magnitude is proportional to  $\epsilon_v$  for that orientation. These radial plots are planar profiles of the specific strain energy surface of a GP zone.

Many profiles of the specific strain energy surface were investigated for the case of a GP zone in an Fe (bcc) lattice. The elastic constants corresponding to Fe are<sup>16</sup>:  $C_{11} = 23.7 \times 10^{11}$  dynes/cm<sup>2</sup>,  $c_{12} = 14.1 \times 10^{11}$  dynes/cm<sup>2</sup>,  $c_{44} = 11.6 \times 10^{11}$  dynes/cm<sup>2</sup>. Figure 1 shows the variation of the specific strain energy upon rotation of the normal vector of a GP zone in the (100) lattice plane. Owing to the four-fold symmetry of the (100)

plane, the plot is symmetric about the  $[011]$  axis. Figure 2 is also an  $\mathcal{E}_v$  surface profile for an Fe lattice. In this case the GP zone normal has been confined to the  $(\bar{1}\bar{1}0)$  lattice plane. As a result of this study of the  $\mathcal{E}_v$  surface in Fe, it was found that the GP zone orientations with the normal vector parallel to a  $\langle 100 \rangle$  direction correspond to minimum values of  $\mathcal{E}_v$ ,  $\langle 111 \rangle$  orientations correspond to maxima on the specific strain energy surface and saddle points are associated with the  $\langle 110 \rangle$  orientations.

Figures 3 and 4 are also plots of the  $(100)$  and  $(\bar{1}\bar{1}0)$  rotation planes, however, the elastic constants have been changed to those corresponding to W. As before, the  $\langle 100 \rangle$  orientations are minima, the  $\langle 111 \rangle$  orientations are maxima and the  $\langle 110 \rangle$  orientations are saddle points on the specific strain energy surface. Comparison of Figs. 2 and 4 shows, however, that the depth and sharpness of the minima are greatly reduced in the case of W.

Figures 5 and 6 again correspond to  $(100)$  and  $(\bar{1}\bar{1}0)$  planar profiles of the specific strain energy surface. The elastic constants in this case are those of an Nb (see Table I) lattice. As in the previous cases, the  $\langle 100 \rangle$ ,  $\langle 110 \rangle$  and  $\langle 111 \rangle$  orientations correspond to extrema on the specific strain energy surface. The roles of the  $\langle 100 \rangle$  and  $\langle 111 \rangle$  orientations, however, are clearly reversed when the elastic constants of Fe or W are replaced by those of Nb.

Table I summarizes the results of calculations involving the elastic constants of a number of metals but retaining the same values of  $\epsilon_p$  and  $\epsilon_n$ . In all cases it was found that the  $\langle 100 \rangle$ ,  $\langle 110 \rangle$  and  $\langle 111 \rangle$  orientations correspond to extrema on the specific strain energy surface. The values of  $\mathcal{E}_v$  for these orientations thus characterize the surface and they

Table I. Numerical results for the critical orientations with fixed values of  $\epsilon_p$  and  $\epsilon_n$ .

Element & Reference	Elastic Constants $10^{11}$ dynes/cm <sup>2</sup>			A	Specific Strain Energy for Indicated Orientation $eV/\text{\AA}^3 \times 10^{-2}$			$\frac{E_v \langle 110 \rangle}{E_v \langle 100 \rangle}$	$\frac{E_v \langle 111 \rangle}{E_v \langle 100 \rangle}$
	$C_{11}$	$C_{12}$	$C_{44}$		$\langle 100 \rangle$	$\langle 110 \rangle$	$\langle 111 \rangle$		
Cu (17)	16.84	12.14	7.54	3.21	0.716	1.455	1.629	2.031	2.274
Ag (17)	12.4	9.34	4.61	3.01	0.479	0.962	1.084	2.010	2.264
Au (17)	18.6	15.7	4.20	2.90	0.487	1.027	1.177	2.110	2.420
Ni (17)	24.65	14.73	12.47	2.51	1.359	2.225	2.430	1.637	1.788
Fe (16)	23.7	14.1	11.6	2.42	1.312	2.103	2.294	1.603	1.748
Al (18)	10.82	6.13	2.85	1.22	0.624	0.693	0.714	1.110	1.144
W (17)	50.1	15.14	19.8	1.13	3.501	3.679	3.735	1.051	1.067
$I_1$ *	24.0	10.0	7.0	1.00	1.602	1.602	1.602	1.000	1.000
$I_2$ *	20.0	12.0	4.0	1.00	1.099	1.099	1.099	1.000	1.000
Mo (17)	46.0	17.6	11.0	0.775	3.129	2.795	2.672	0.893	0.854
Cr (19)	35.0	6.78	10.08	0.714	2.44	2.17	2.06	0.889	0.844
Nb (20)	24.6	13.4	2.87	0.813	1.461	1.042	0.879	0.714	0.602

$I_1$  and  $I_2$  are two hypothetical isotropic materials with cubic lattices.

are presented in Table I.

Perhaps the most significant general feature of this table is the relationship between the elastic anisotropy parameter A, defined as:

$$A = \frac{2C_{44}}{C_{11} - C_{12}},$$

and the orientation corresponding to the minimum specific strain energy.

For the particular values of  $\epsilon_p$  and  $\epsilon_n$  used in these calculations, the  $\langle 100 \rangle$  orientations are minima when  $A > 1$  and the  $\langle 111 \rangle$  orientations are minima for  $A < 1$ . This is precisely the relationship found by Schwellinger et al<sup>10</sup> in their study of two-dimensionally infinite misfitting plates.

For the purposes of this paper, however, it is not yet a general statement since the shape of the specific strain energy surface may also depend on the values of the transformation parameters.

#### B. Dependence of the Specific Strain Energy in $\epsilon_p$ and $\epsilon_n$ .

That  $\mathcal{E}_v$  for a particular orientation of a GP zone must depend on the transformation parameters is evident from the limiting case. As  $\epsilon_p$  and  $\epsilon_n$  go to zero,  $\mathcal{E}_v$  must also go to zero. For all sets of elastic constants listed in Table I, however, it has been found that the ratios  $\mathcal{E}_v \langle 110 \rangle / \mathcal{E}_v \langle 100 \rangle$  and  $\mathcal{E}_v \langle 111 \rangle / \mathcal{E}_v \langle 100 \rangle$  are independent of the values of the parameters  $\epsilon_p$  and  $\epsilon_n$ . This is significant because it shows, for all of the cases in Table I, that the salient features of the specific strain energy surface are independent of the parameters characterizing the transformation. For these cases the shape of the  $\mathcal{E}_v$  surface depends only on the elastic properties of the matrix phase.

## IV. DISCUSSION

A. Relationship Between Minimum Energy Orientations and Elastic Anisotropy

In the previous section it was observed that for all cases investigated, the shape of the specific strain energy surface is independent of the transformation parameters  $\epsilon_p$  and  $\epsilon_a$ . Since either the  $\langle 111 \rangle$  or  $\langle 100 \rangle$  orientations correspond to the minimum value of  $\mathcal{E}_v$  in all cases investigated (except for the totally degenerate case when  $A = 1$ ), the ratio  $\mathcal{E}_v \langle 111 \rangle / \mathcal{E}_v \langle 100 \rangle$  reflects an essential feature of the surface. Fig. 7 is a plot of this ratio vs the anisotropy parameter  $A$ . Inferring from Fig. 7 that this approximate linear relationship is valid in all cases, one observes that for  $A > 1$ , the ratio  $\mathcal{E}_v \langle 111 \rangle / \mathcal{E}_v \langle 100 \rangle$  is also greater than one, implying that the  $\langle 100 \rangle$  orientations are minima on the  $\mathcal{E}_v$  surface. For  $A < 1$  this ratio is less than one so that the  $\langle 111 \rangle$  orientations correspond to minima on the  $\mathcal{E}_v$  surface. This relationship, originally proposed by Schwelling et al.<sup>10</sup>, is thus valid for all disk-shaped coherent inclusions. One may conclude that if the strain energy is the only configuration dependent parameter, disk-shaped GP zones will form preferentially on the  $\langle 100 \rangle$  matrix planes if  $A > 1$  and on the  $\langle 111 \rangle$  planes if  $A < 1$ . Simple calculations for GP zones of typical size, however, indicate that an additional interfacial energy term would be important if the interfacial energy density exceeded a few hundred ergs/cm<sup>2</sup>.

B. The Case for Al-Cu

The Al-Cu binary alloys are the basis of many technologically important alloys, meriting special consideration of this case. The elastic constants of Al are given in Table I and the transformation parameters computed from lattice parameter measurements<sup>15</sup> are  $\epsilon_p = -0.108$  and  $\epsilon_a =$



0.0595. Vigier et al<sup>21</sup> report that the GP zones in an Al-11.74 a/o Cu alloy have a diameter of about 80 Å and the pre-transformation thickness of a monolayer may be taken as half of an Al lattice parameter, about 2 Å.

A plot of the variation of the strain energy of a GP zone of the above dimensions with the normal vector confined to the (100) plane is shown in Fig. 8. Figure 9 is a similar plot for a GP zone in Al-Cu but the rotation plane is (110) in this case. From these plots it is seen that the <100> orientations correspond to the minimum strain energy and it is interesting to note that this is also the observed GP zone orientation in Al-Cu alloys.<sup>1</sup> In Fig. 8 and 9 the minima are broad and shallow (A being only slightly greater than one) and from this, one might expect some variation in the observed orientations of the GP zones. Since no variation is observed, one could speculate that the additional interfacial energy or strain field interactions might be important in this case.

In Al - 1.74 a/o Cu alloys, GP zone densities of the order of  $5 \times 10^{17}$  cm<sup>-3</sup> are commonly observed.<sup>1</sup> Assuming that all of the GP zones are in (or very near to) minimum strain energy orientation and ignoring strain field interactions, the strain energy associated with the GP zones in this alloy is 8.6 cal per mole alloy. Comparing this with other energy changes which accompany GP zone formation,<sup>21-22</sup> it is seen to be a plausible value.

### C. The Case for Cu-Be

Similar calculations may be made for another important alloy in which disk-shaped GP zones are observed, Cu-Be. The elastic constants for Cu are given in Table I and values of  $\epsilon_p$  and  $\epsilon_n$  of -0.118 and -0.0433 respectively were calculated from lattice parameter measurements.<sup>15</sup> For a Cu-12.37 a/o

Be alloy,<sup>6</sup> the observed GP zone diameter is about 60A and the thickness is taken as one half a Cu lattice spacing, 1.85A.

Plots of the variation of the strain energy when a GP zone normal is confined to the (100) and ( $\bar{1}\bar{1}0$ ) planes are shown in Figs. 10 and 11, respectively. Again the minimum strain energy orientation is  $\langle 100 \rangle$  and this corresponds precisely with the observed GP zone orientation in this alloy.<sup>1</sup> Comparison of Figs. 8-11 re-emphasizes the dependence of the shape of the strain energy surface on the anisotropy parameter A. Unlike the case for Al-Cu, the minima in Figs. 10 and 11 are fairly sharp and deep so one would expect other factors to be less necessary in suppressing variations in the observed orientations of GP zones in this alloy.

#### D. General Discussion

One striking feature of age hardening alloy systems is the apparent ease with which GP zones form in some alloys but not in others. In the two cases considered in the previous paragraphs, disk-shaped GP zones form quite readily. Such GP zones have been observed in other alloys but they do not appear to form as easily as one might expect after examination of the Al-Cu and Cu-Be alloys. Consideration of Table I may permit some speculation on this point.

Supersaturating binary alloys exist with all of the elements listed in Table I as the base metal. Comparing the minimum values of  $\epsilon_v$  for the various metals, it is seen that the values for Al and Cu are among the lowest of all of the elements listed. Since the strain energy associated with the coherent clusters contributes to the barrier to nucleation and growth, the low values of  $\epsilon_v$  for Al and Cu are well correlated with the apparent ease with which GP zones form in these alloys. Similarly, it may

be noted that the minimum value of  $\epsilon_v$  for Fe is comparatively large and, indeed, disk-shaped coherent precipitates are not an important strengthening mechanism in iron based alloys. At present, the energetics of precipitation processes are not well documented so it is impossible to determine the relative importance of the strain energy contribution to the barrier to GP zone formation. Further investigation in this area is clearly indicated, however, in order to expand the understanding and applicability of this strengthening mechanism.

#### V. CONCLUSIONS

1. An approximate expression for the specific strain energy of an isolated disk-shaped inclusion is obtained from Khachatryan's solution to the general problem. Numerical results are presented for a number of metallic elements with varying elastic properties.
2. It is found that the shape of the specific strain energy surface is independent of the transformation parameters.
3. The relationship between the anisotropy parameter  $A$  and the GP zone orientation of minimum strain energy proposed by Schwellinger et al.<sup>10</sup> is verified. An approximate linear relationship between the ratio of the strain energies for the  $\langle 111 \rangle$  and  $\langle 100 \rangle$  and the parameter  $A$  is observed.
4. Profiles of strain energy surfaces are presented for Al-Cu and Cu-Be alloys. The minimum energy orientations are identical with experimentally observed orientations.

ACKNOWLEDGMENTS

The author is deeply indebted to Professor E. R. Parker and Professor J. W. Morris, Jr. for their interest and encouragement.

This work was done under the auspices of the U. S. Atomic Energy Commission.

REFERENCES

1. A. Kelly and R. B. Nicholson, Prog. Mat. Sci. 10, 149 (1963).
2. H. Warlimont, Electron Microscopy and Structure of Materials, G. Thomas (ed). Univ. of Cal. Press, 1972 p.505.
3. R. B. Nicholson and J. Nutting, Acta Met. 9, 332 (1961).
4. V. A. Phillips and J. D. Livingston, Phil. Mag. 7, 969 (1962).
5. V. A. Phillips, Acta Met. 21, 219 (1973).
6. V. A. Phillips and L. Tanner, Acta Met. 21, 441 (1973).
7. J. Higgins and P. Wilkes, Phil. Mag. 25, 599 (1972).
8. W. B. Grupen and G. Sines, Report 64-10, Eng. Dept., Univ. of California.
9. A. Khachaturyan and V. Hairapetyan, Phys. Stat. Sol. 57, 801 (1973).
10. P. Schwellinger, H. Leamy and H. Warlimont, Acta Met. 19, 421 (1971).
11. J. D. Eshelby, Proc. Roy. Soc. A 241, 376 (1957).
12. A. G. Khachaturyan, Soviet Phys. - Solid State. 8, 2163 (1967).
13. K. Toman, Acta Cryst. 13, 60 (1960).
14. V. Gerold, Z. Metallk. 45, 593 & 599 (1954).
15. W. Pearson, Handbook of Lattice Spacings and Structures of Metals and Alloys, Vol. 1. Pergamon Press, New York, (1958).
16. W. Mason, Piezoelectric Crystals and Their Application to Ultrasonics. Van Nostrand, New York, (1950).
17. H. B. Huntington, Solid State Phys. 7, 213 (1958).
18. P. M. Sutton, Phys. Rev. 91, 816 (1953).
19. D. Bolef and J. deKlerk, Phys. Rev. 129, 1063 (1963).
20. D. Bolef, J. Appl. Phys. 32, 100 (1961).
21. P. Vigier et al, Mem. Sci. Rev. Met. 69, 51 (1972).
22. W. Desorbo, H. Treafitis and D. Turnbull, Acta Met. 6, 401 (1958).

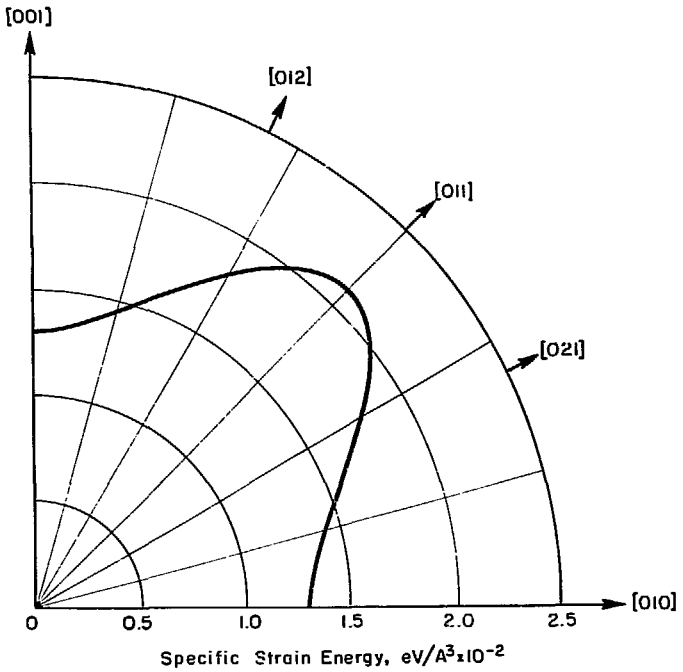
FIGURE CAPTIONS

- Fig. 1. Variation of the specific strain energy of a GP zone in an Fe lattice where the normal vector has been confined to the (100) plane.
- Fig. 2. Variation of the specific strain energy of a GP zone in an Fe lattice where the normal vector has been confined to the (1 $\bar{1}$ 0) plane.
- Fig. 3. Variation of the specific strain energy of a GP zone in a W lattice where the normal vector has been confined to the (100) plane.
- Fig. 4. Variation of the specific strain energy of a GP zone in a W lattice where the normal vector has been confined to the (1 $\bar{1}$ 0) plane.
- Fig. 5. Variation of the specific strain energy of a GP zone in an Nb lattice where the normal vector has been confined to the (100) plane.
- Fig. 6. Variation of the specific strain energy of a GP zone in an Nb lattice where the normal vector has been confined to the (1 $\bar{1}$ 0) plane.
- Fig. 7. The relationship between the ratio  $\epsilon_v\langle 111 \rangle / \epsilon_v\langle 100 \rangle$  and the elastic anisotropy parameter A.
- Fig. 8. Variation of the strain energy of a GP zone in an Al-Cu alloy where the normal vector has been confined to the (100) plane.
- Fig. 9. Variation of the strain energy of a GP zone in an Al-Cu alloy where the normal vector has been confined to the (1 $\bar{1}$ 0) plane.

Fig. 10. Variation of the strain energy of a GP zone in a Cu-Be alloy where the normal vector has been confined to the (100) plane.

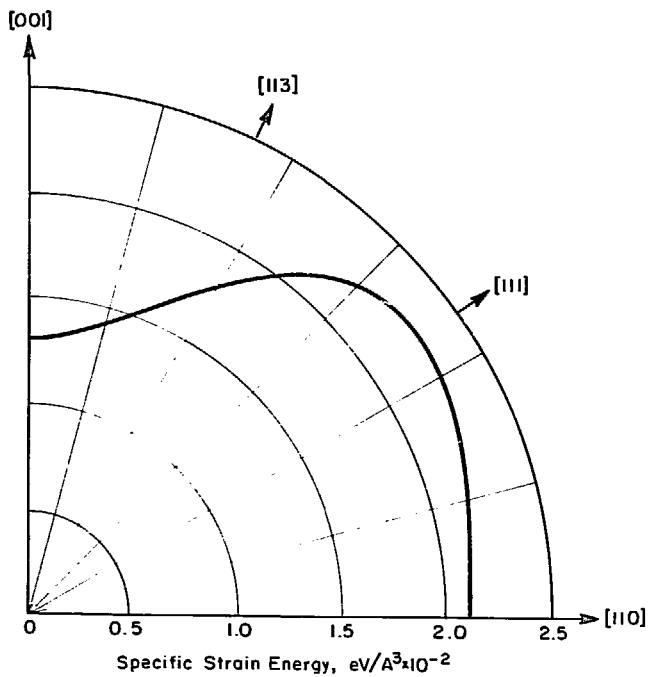
Fig. 11. Variation of the strain energy of a GP zone in a Cu-Be alloy where the normal vector has been confined to the (110) plane.





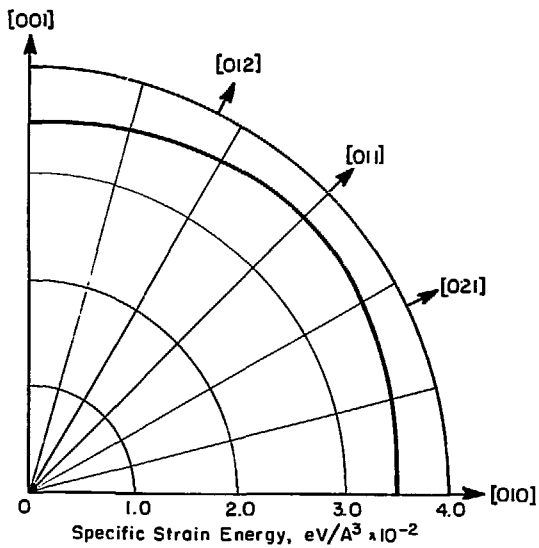
XBL 749-7327

Fig. 1



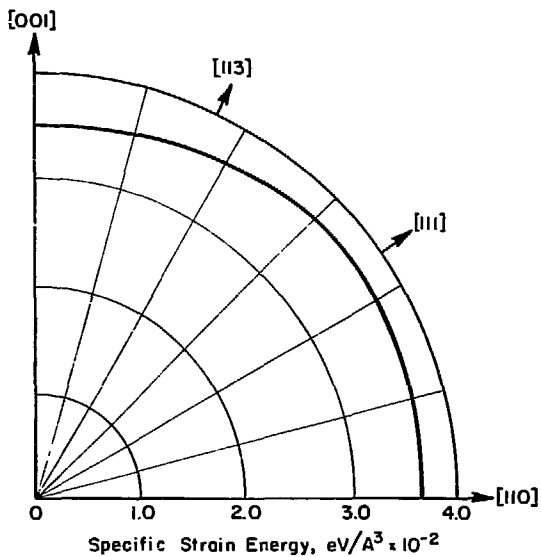
XBL 749-7328

Fig. 2



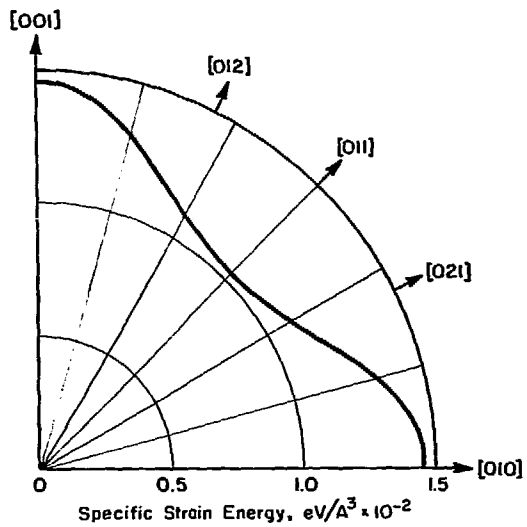
XBL7411-7580

Fig. 3



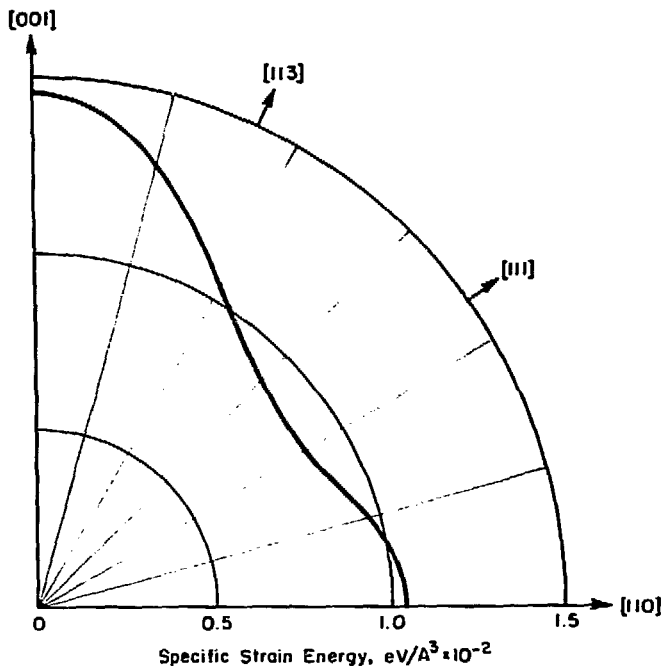
XBL 7411-7579

Fig. 4



XBL 7411-7577

Fig. 5



XBL 749-7329

Fig. 6

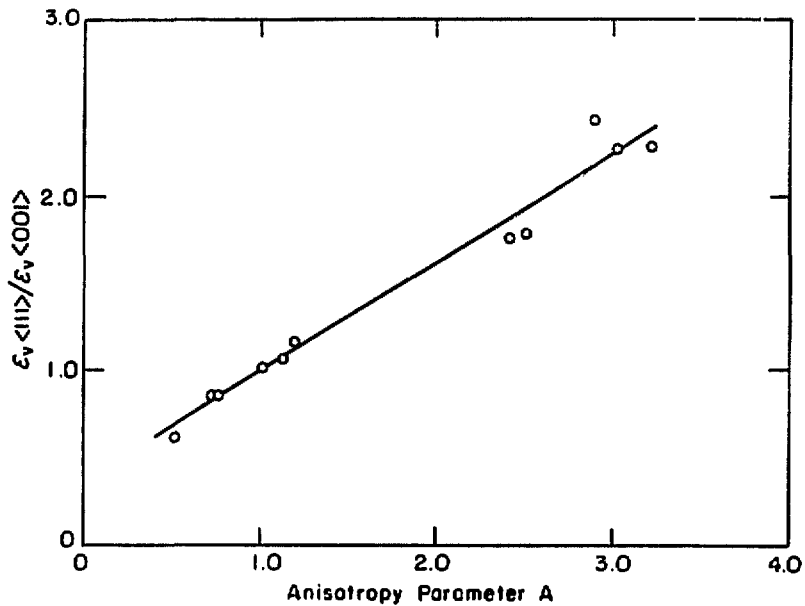
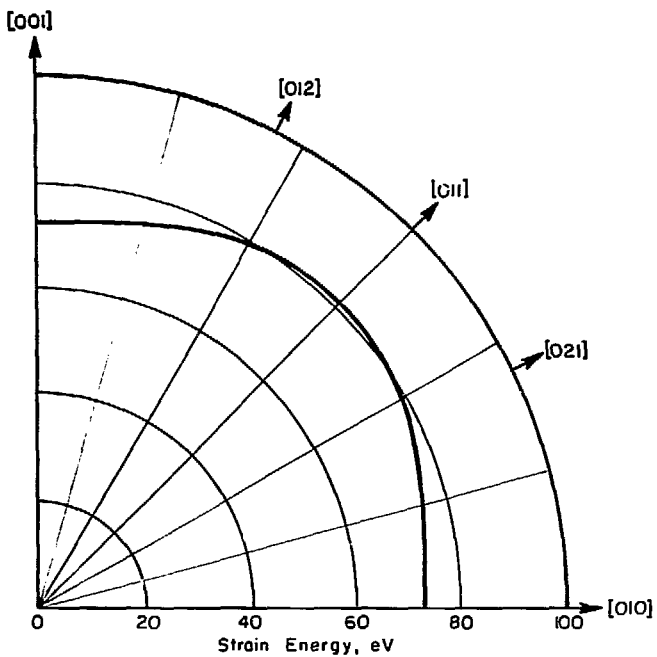


Fig. 7

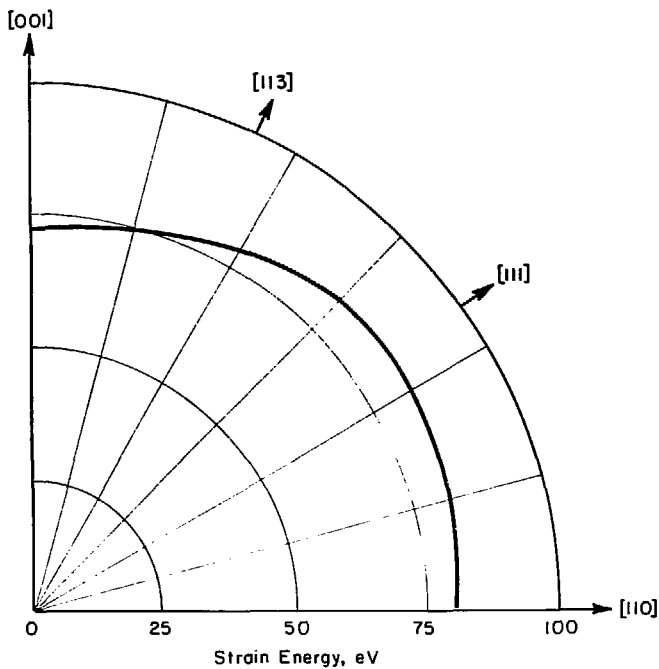
XBL 749-7 330



XBL 7411-7576

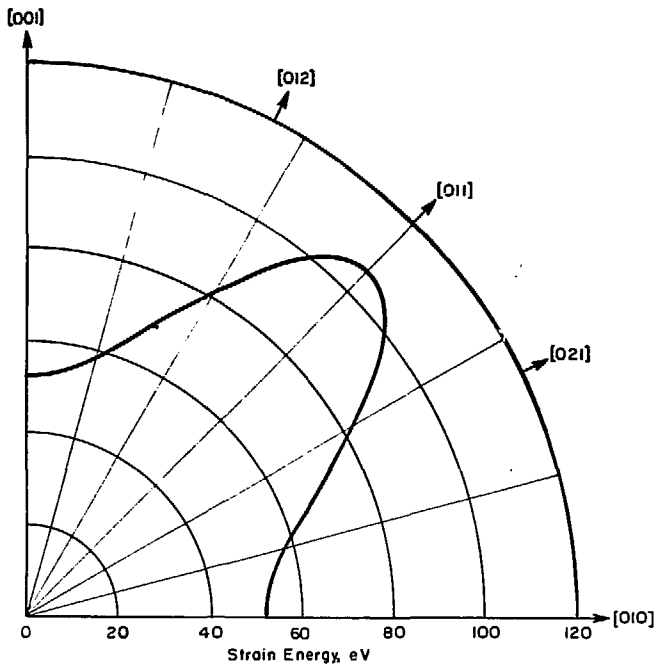
Fig. 8





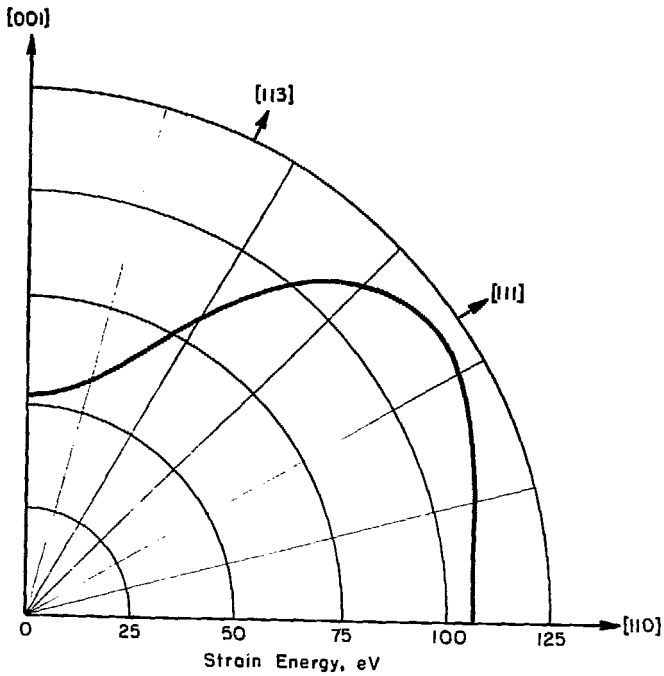
XBL749-7331

Fig. 9



XBL 7411-7578

Fig. 10



XBL 749-7332

Fig. 11